

Turbulence with combined stratification and rotation: Limitations of Corrsin's hypothesis

F. Nicolleau*

Mechanical Engineering, The University of Sheffield, Mapping Street, Sheffield, S1 3JD, United Kingdom

G. Yu

Department of Engineering, Queen Mary, University of London, Mile End Road, E1 4NS, London, United Kingdom

(Received 22 February 2007; published 5 December 2007)

The properties of one-particle and particle-pair diffusion in rotating and stratified turbulence are studied by applying the rapid distortion theory to a kinematic simulation of the Boussinesq equation with a Coriolis term. We discuss the simplified Corrsin hypothesis and restrict the validity of its predictions to pure rotation. We emphasize the existence of two τ regimes driven by very different physics when rotation is present. Particular attention is given to the locality-in-scale hypothesis for two-particle diffusion in both the horizontal and the vertical directions.

DOI: [10.1103/PhysRevE.76.066302](https://doi.org/10.1103/PhysRevE.76.066302)

PACS number(s): 47.27.tb, 47.55.Hd

I. INTRODUCTION

Rapidly rotating turbulence with or without stratification is to be found in many geophysical or industrial flows. In this paper, the flow field is described by the simplified Boussinesq approximation based on rapid distortion theory (RDT). We use the kinematic simulation (KS) discussed in [1] (see references therein). More details of the RDT model for stratified and rotating turbulence can also be found in [2]. This paper addressed the question of the validity of Corrsin's simplified hypothesis, which states the equivalence between Eulerian and Lagrangian correlations. Vertical correlations were found to follow this postulate, but not the horizontal ones.

The properties of one-particle and particle-pair diffusion in high-Reynolds-number and low-Froude-number stably stratified nondecaying turbulence were presented in detail in [3]. The properties of one-particle and particle-pair diffusion in rotating and stratified turbulence were studied in [1].

KSs are a very good tool for understanding the role of the linear terms in the Boussinesq equation, and our results show that these terms can explain many features concerning one- and two-particle diffusion. Our approach is to understand their role fully before moving on to more complex models.

In kinematic simulation, in order to derive the Lagrangian trajectories, one has to integrate an *a priori* Eulerian velocity field

$$\frac{d\mathbf{x}}{dt} = \mathbf{u}(\mathbf{x}, t) \quad (1)$$

knowing the initial conditions for the fluid element (alias particle in this paper) \mathbf{x}_0 and $\mathbf{u}(\mathbf{x}_0, 0)$. After its release the particle will experience the action of all scales, and the KS must therefore retain information about all scales, not only large ones. Hence, in a KS the velocity field $\mathbf{u}(\mathbf{x}, t)$ is modeled with the same accuracy from the largest down to the smallest scale.

KSs were first developed for homogeneous isotropic turbulence where incompressibility and an energy power law

spectrum were prescribed (e.g., [4–6], and references therein). It appears from [7–9] that for many Lagrangian properties no particular time dependence needs to be introduced, and a “frozen” three-dimensional (3D) Eulerian velocity field can generate many Lagrangian properties of the turbulence. The three-dimensionality of streamlines ensures all the necessary time decorrelations to obtain the ballistic, random walk, and Richardson regimes for particle pairs initially separated by η , the Kolmogorov length scale [10].

For stably stratified flows, an analysis of the Lagrangian velocity-time correlation [2,3,11] shows that its time dependence is far more complex than for homogeneous isotropic turbulence and is crucial for the prediction of particle diffusion along the axis of stratification.

Comparisons of KS results with RDT and direct numerical simulation (DNS) results can be found in [2]; additional DNS results can also be found in [12].

In this paper, we consider a flow subjected to both stratification and rotation characterized, respectively, by a Brünt-Väissälä frequency N and a rotation rate Ω . We investigate one- and two-particle diffusion along the vertical axis and in the plane orthogonal to the vertical axis. The rotation Ω , gravity, and mean density gradient are all in the direction of the vertical axis, referred to as the third axis throughout this paper: $\Omega = (0, 0, \Omega)$, $\mathbf{g} = (0, 0, -g)$. The stratification is stable and the turbulence nondecaying.

In Sec. II we introduce the KS model and its notations, and also the locality-in-scale assumption as it is to be discussed in this paper. Results for the combined effect of stratification and rotation are given in Sec. III for one-particle statistics and in Sec. IV for particle-pair statistics. Section V summarizes this paper's main conclusions.

II. EQUATIONS

A. The Boussinesq assumption

Our KS is based on the Boussinesq assumption. We consider a stably stratified fluid at static equilibrium, with pressure $p(x_3)$ and density $\rho(x_3)$ varying only in the direction of stratification, which is along the vertical axis x_3 (see Fig. 1).

*F.Nicolleau@Sheffield.ac.uk

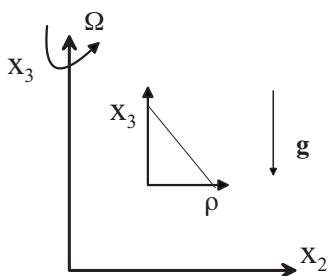


FIG. 1. Stratification and rotation direction.

Hence $dp/dx_3 = -\rho g$ where $\mathbf{g} = (0, 0, -g)$ is the gravitational acceleration, and we set $Ro = 0.00035$ in Cartesian coordinates. Under the Boussinesq approximation the perturbation density ρ' is assumed much smaller than the density ρ so that

$$\frac{D}{Dt} \Theta = -u_3 \frac{1}{\rho} \frac{d\rho}{dx_3}, \quad (2)$$

where $\Theta = \rho'/\rho$. The rotation intervenes as a Coriolis term $2\mathbf{\Omega} \times \mathbf{u}$ superimposed on the stratified flow dynamics:

$$\frac{D\mathbf{u}}{Dt} = -\frac{1}{\rho} \nabla p' + \Theta \mathbf{g} - 2\mathbf{\Omega} \times \mathbf{u}, \quad (3)$$

with $\mathbf{\Omega}$ the rotation vector. In this paper the study is limited to a rotation in the direction of stratification, that is, $\mathbf{\Omega} = (0, 0, \Omega)$. As in [3], for the sake of simplicity we omit terms describing molecular diffusion and viscosity. Though there is no theoretical difficulty in incorporating these terms, in practice they make computations rather cumbersome. The perturbation velocity $\mathbf{u}(\mathbf{x}, t)$ is also assumed incompressible:

$$\nabla \cdot \mathbf{u} = 0. \quad (4)$$

B. Linearized Boussinesq equations with rotation

Consider an initial velocity field $\mathbf{u}(\mathbf{x}, 0)$ with spatial fluctuations over a wide range of length scales, the smallest of these length scales being η . In the limit where the microscale Froude number and the microscale Rossby number are much smaller than 1, i.e., $Fr_\eta \equiv u(\eta)/N\eta \ll 1$ and $Ro_\eta \equiv u(\eta)/\Omega\eta \ll 1$ [where $u(\eta)$ is the characteristic initial velocity fluctuation at scale η], and in the case where $u(\eta)$ corresponds to the smallest characteristic time scale in the initial flow, the Eulerian Boussinesq equations (2) and (3) may be approximated by their linear counterparts

$$\frac{\partial}{\partial t} \Theta = -u_3 \frac{1}{\rho} \frac{d\rho}{dx_3}, \quad (5)$$

$$\frac{\partial}{\partial t} \mathbf{u} = -\frac{1}{\rho} \nabla p' + \Theta \mathbf{g} - 2\mathbf{\Omega} \times \mathbf{u}. \quad (6)$$

We use the Fourier transform $\tilde{\mathbf{u}}(\mathbf{k}, t)$ of $\mathbf{u}(\mathbf{x}, t)$ to solve Eqs. (5) and (6) so that the incompressibility constraint (4) is transformed into $\mathbf{k} \cdot \tilde{\mathbf{u}}(\mathbf{k}, t) = 0$, while the pressure field gradient is transformed into a vector parallel to \mathbf{k} in Fourier space. Letting \mathbf{e}_3 be the unit vector in the direction of stratification

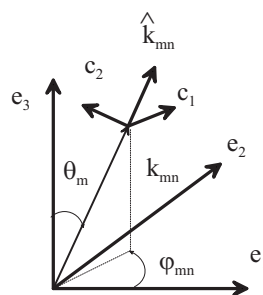


FIG. 2. Craya-Herring frame and Fourier space discretization.

and $\mathbf{e}_1, \mathbf{e}_2$ two unit vectors normal to each other and to \mathbf{e}_3 (so that $\mathbf{x} = x_1 \mathbf{e}_1 + x_2 \mathbf{e}_2 + x_3 \mathbf{e}_3$ and $\mathbf{g} = -g \mathbf{e}_3$), the Craya-Herring frame (see Fig. 2) is given by the unit vectors $\hat{\mathbf{k}} = \mathbf{k}/k$, $\mathbf{c}_1 = (\mathbf{e}_3 \times \mathbf{k})/(\mathbf{e}_3 \times \mathbf{k})$ and $\mathbf{c}_2 = (\mathbf{k} \times \mathbf{c}_1)/(\mathbf{k} \times \mathbf{c}_1)$. In the Craya-Herring frame, the Fourier-transformed velocity field $\tilde{\mathbf{u}}(\mathbf{k}, t)$ lies in the plane defined by \mathbf{c}_1 and \mathbf{c}_2 , i.e.,

$$\tilde{\mathbf{u}}(\mathbf{k}, t) = \tilde{v}_1(\mathbf{k}, t) \mathbf{c}_1 + \tilde{v}_2(\mathbf{k}, t) \mathbf{c}_2, \quad (7)$$

and is therefore decoupled from the pressure fluctuations, which are along \mathbf{k} . This decomposition is generic for any divergence-free velocity field, and related to a classical toroidal-poloidal one in physical space, where toroidal refers to the component $\tilde{v}_1(\mathbf{k}, t) \mathbf{c}_1$ whereas poloidal refers to the component $\tilde{v}_2(\mathbf{k}, t) \mathbf{c}_2$. The toroidal mode is purely horizontal, whereas the poloidal mode will yield a horizontal and a vertical component.

Incompressible solutions of Eqs. (5) and (6) in Fourier space and in the Craya-Herring frame are [13]

$$\begin{aligned} \tilde{v}_1(\mathbf{k}, t) = & \frac{\sigma_s^2}{\sigma^2} \tilde{v}_1(\mathbf{k}, 0) - \frac{\sigma_r g \sin \theta}{\sigma^2} \tilde{\Theta}(\mathbf{k}, 0) + \left(\frac{\sigma_r^2}{\sigma^2} \tilde{v}_1(\mathbf{k}, 0) \right. \\ & \left. + \frac{\sigma_r g \sin \theta}{\sigma^2} \tilde{\Theta}(\mathbf{k}, 0) \right) \cos \sigma t + \frac{\sigma_r}{\sigma} \tilde{v}_2(\mathbf{k}, 0) \sin \sigma t, \end{aligned} \quad (8)$$

$$\begin{aligned} \tilde{v}_2(\mathbf{k}, t) = & \tilde{v}_2(\mathbf{k}, 0) \cos \sigma t - \left(\frac{\sigma_r}{\sigma} \tilde{v}_1(\mathbf{k}, 0) \right. \\ & \left. + \frac{g \sin \theta}{\sigma} \tilde{\Theta}(\mathbf{k}, 0) \right) \sin \sigma t, \end{aligned} \quad (9)$$

$$\begin{aligned} \tilde{\Theta}(\mathbf{k}, t) = & -\frac{N \sigma_r \sigma_s}{g \sigma^2} \tilde{v}_1(\mathbf{k}, 0) + \frac{\sigma_r^2}{\sigma^2} \tilde{\Theta}(\mathbf{k}, 0) + \frac{N \sigma_s}{g \sigma^2} (\sigma_r \tilde{v}_1(\mathbf{k}, 0) \\ & + g \sin \theta \tilde{\Theta}(\mathbf{k}, 0)) \cos \sigma t + \frac{N \sigma_s}{g \sigma} \tilde{v}_2(\mathbf{k}, 0) \sin \sigma t, \end{aligned} \quad (10)$$

where $\theta = \theta(\mathbf{k})$ is the angle between \mathbf{k} and \mathbf{e}_3 , $\sigma_r = 2\Omega \cos \theta$, $\sigma_s = N \sin \theta$, $\sigma = \sqrt{\sigma_r^2 + \sigma_s^2}$, and the initial conditions are $\tilde{v}_1(\mathbf{k}, 0)$, $\tilde{v}_2(\mathbf{k}, 0)$, and $\tilde{\Theta}(\mathbf{k}, 0)$.

In this paper the study is limited to the case $\tilde{\Theta}(\mathbf{k}, 0) = 0$ (zero initial potential energy), in which case Eqs. (8)–(10) become

$$\tilde{v}_1(\mathbf{k}, t) = \frac{\sigma_s^2}{\sigma^2} \tilde{v}_1(\mathbf{k}, 0) + \frac{\sigma_r^2}{\sigma^2} \tilde{v}_1(\mathbf{k}, 0) \cos \sigma t + \frac{\sigma_r}{\sigma} \tilde{v}_2(\mathbf{k}, 0) \sin \sigma t, \quad (11)$$

$$\tilde{v}_2(\mathbf{k}, t) = \tilde{v}_2(\mathbf{k}, 0) \cos \sigma t - \frac{\sigma_r}{\sigma} \tilde{v}_1(\mathbf{k}, 0) \sin \sigma t, \quad (12)$$

$$\begin{aligned} \tilde{\Theta}(\mathbf{k}, t) = & -\frac{N \sigma_r \sigma_s}{g \sigma^2} \tilde{v}_1(\mathbf{k}, 0) + \frac{N \sigma_s \sigma_r}{g \sigma^2} \tilde{v}_1(\mathbf{k}, 0) \cos \sigma t \\ & + \frac{N \sigma_s}{g \sigma} \tilde{v}_2(\mathbf{k}, 0) \sin \sigma t. \end{aligned} \quad (13)$$

It is worth here introducing [2]'s approach (see also [14]): stably stratified turbulence and rotating turbulence can be considered as the superposition of a vortex mode and an internal wave mode. The vortex and internal wave modes are linearly independent, linked only through nonlinear terms in (3). Linear dynamics affects only the wave mode, and consists of periodic exchanges of energy between the wave part of the velocity (identical to the poloidal component only for pure stratification) and the buoyancy field, if stratification is present. In the case of pure rotation, only kinetic energy is concerned, and inertial waves exchange energy between poloidal and toroidal components of the velocity field.

C. KS velocity field

We generalize [3]'s KS velocity field for stratified turbulence. Here, a homogeneous isotropic turbulent field is subjected to rotation with or without stratification. The KS model of turbulent diffusion in rotating or/and stratified non-decaying turbulence consists in solving

$$\frac{d\mathbf{x}}{dt} = \mathbf{u}(\mathbf{x}(t), t) \quad (14)$$

to obtain an ensemble of Lagrangian trajectories $\mathbf{x}(t)$ from the velocity field,

$$\begin{aligned} \mathbf{u}(\mathbf{x}, t) = & 2\pi \text{Re} \left\{ \sum_{n=1}^{N_k} \sum_{m=1}^{M_\theta} k_n^2 \sin \theta_m \Delta k_n \Delta \theta_m e^{ik_{mn} \cdot \mathbf{x}} \right. \\ & \left. \times [\tilde{v}_1(\mathbf{k}_{mn}, t) \mathbf{c}_1(\mathbf{k}_{mn}) + \tilde{v}_2(\mathbf{k}_{mn}, t) \mathbf{c}_2(\mathbf{k}_{mn})] \right\}, \end{aligned} \quad (15)$$

where Re stands for the real part, $\tilde{v}_1(\mathbf{k}_{mn}, t)$ obeys Eq. (11), and $\tilde{v}_2(\mathbf{k}_{mn}, t)$ Eq. (12). $\tilde{v}_1(\mathbf{k}_{mn}, 0)$ and $\tilde{v}_2(\mathbf{k}_{mn}, 0)$ are specified initial conditions randomly chosen in accordance with an energy spectrum $E(k)$ that has a $-5/3$ large-wave-number scaling, that is,

$$E(k) \begin{cases} \sim k^{-5/3} & \text{for } k_1 \leq k \leq k_{N_k} \equiv 2\pi/\eta, \\ = 0 & \text{otherwise.} \end{cases} \quad (16)$$

The spectrum is characterized by the rms value of the velocity fluctuation

$$u'^2 = \frac{2}{3} \int E(k) dk, \quad (17)$$

the integral length scale

$$L = \frac{3\pi}{4} \frac{\int k^{-1} E(k) dk}{\int E(k) dk} \quad (18)$$

of the initial isotropic turbulence, and the Kolmogorov length scale η . We also introduce t_d , the eddy turnover time associated with L and u' , as follows:

$$t_d = \frac{L}{u'}, \quad (19)$$

and τ_η , the characteristic time associated with the inner (viscosity simulating) length scale:

$$\tau_\eta = \left(\frac{\eta}{L} \right)^{2/3} t_d. \quad (20)$$

In this paper, we choose the values $M_\theta=20$ and $N_k=50$ for the cases with both stratification and rotation. For pure rotation it was found that a refined discretization of the angles θ is needed, and we chose $M_\theta=100$ and $N_k=30$.

Velocity correlations were tested against RDT and DNS results. They have shown satisfactory agreement for most cases $0 \leq 2\Omega/N \leq \infty$ [see [2] for details].

For the sake of simplicity we introduce the following notations:

$$\tau = t - t_0,$$

$$\zeta_i(\tau) = x_i(t) - x_i(t_0),$$

$$\Delta_i(\tau) = x_i^1(t) - x_i^2(t),$$

$$\Delta_0 = |\mathbf{x}^1(0) - \mathbf{x}^2(0)|,$$

$$\Delta_i^r(\tau) = [x_i^1(t) - x_i^1(t_0)] - [x_i^2(t) - x_i^2(t_0)],$$

$$\delta_i(\tau) = \sqrt{\langle \Delta_i^r(t)^2 \rangle},$$

$$\delta_i^v(\tau) = \sqrt{\langle \Delta_i^v(t)^2 \rangle}, \quad (21)$$

where t_0 is the time of release of the particle, x_i is the i th component of the particle's position vector \mathbf{x} , \mathbf{x}^1 refers to the first particle of the particle pair and \mathbf{x}^2 to the second particle of the pair. The subscripts h and v when they are substituted for i indicate, respectively, horizontal and vertical properties. The strength of the stratification is characterized by the Froude number Fr:

$$\text{Fr} = \frac{u'}{LN}, \quad (22)$$

and the strength of the rotation by the Rossby number Ro:

$$Ro = \frac{u'}{2L\Omega}. \quad (23)$$

When rotation is superimposed on stratification or vice versa, different flow structure interactions result in different behaviors for both one- and two-particle diffusions. A parameter defined as

$$B = \frac{Fr}{Ro} = \frac{2\Omega}{N} \quad (24)$$

is used to classify the turbulence. If $B > 1$ the turbulence is called rotation dominated whereas it is referred to as stratification dominated if $B < 1$.

D. The locality-in-scale hypothesis

The locality-in-scale assumption was introduced in [15] and [16], according to which the pair diffusivity $(d/dt)\langle\Delta^2\rangle$ is mainly sensitive to eddies of size $\delta = \sqrt{\langle\Delta^2\rangle}$. For a turbulence spectrum $E(k) \sim k^{-5/3}$, it can easily be shown that this assumption leads to

$$\frac{d}{dt}\langle\Delta^2\rangle = \beta u' \eta \left(\frac{L}{\eta}\right)^{-1/3} \left(\frac{\delta}{\eta}\right)^{4/3} \quad (25)$$

and, equivalently, to

$$\langle\Delta^2(\tau)\rangle = G_\Delta \epsilon \tau^3 \quad (26)$$

where we neglect initial separation terms [6,17]. For an anisotropic flow we can define a coefficient β_h based on the horizontal diffusivity as follows:

$$\frac{d}{dt}\langle\Delta_h^2\rangle = \beta_h u' \eta \left(\frac{L}{\eta}\right)^{-1/3} \left(\frac{\delta_h}{\eta}\right)^{4/3}. \quad (27)$$

In [10] it was shown that the best way to estimate Richardson's locality assumption is to study Richardson's coefficient β defined by Eq. (25). Though the diffusivity $(d/dt)\langle\Delta^2\rangle$ and the pair rms separation δ are functions of time, time does not appear explicitly in Eq. (25), which simplifies greatly the study of the effect of the initial condition and enables clear conclusions on the validity of the locality-in-scale assumption. If β is constant, then the locality-in-scale assumption is verified, otherwise β will measure the departure from this assumption. We also define χ_i (where $i = 1, 2, 3$ for pair diffusion in different directions) as the range of δ/η over which the locality assumption is observed. (We discussed in [1] the reasons for extending this interpretation to stratified or rotating turbulence.)

III. ONE-PARTICLE DIFFUSION IN STRATIFIED AND ROTATING TURBULENCE

For different values of B , the results of one-particle diffusion are compared to those obtained in purely stratified turbulence and purely rotating turbulence. The discussion is carried out in terms of $B < 1$ and $B > 1$. In each case, the turbulence parameters u' , L , η , and N or Ω (as long as B is kept constant) are varied. The different cases are reported in Table I. The one-particle horizontal and vertical diffusions

TABLE I. Different cases studied for particle diffusion in stratified and rotating turbulence.

Case	Ω	N	L	u'	$1/\eta$	Δ_0/η	B
A	0	500	1	0.35	12.5	1	0
B	100	1000	1	0.35	12.5	1	0.2
C	100	1000	2	0.35	12.5	1	0.2
D	100	1000	1	0.175	12.5	1	0.2
E	100	1000	1	0.35	6.5	1	0.2
F	200	2000	1	0.35	12.5	1	0.2
G	100	1000	1	0.35	12.5	0.02	0.2
H	100	1000	1	0.35	12.5	0.2	0.2
I	100	1000	1	0.35	12.5	5	0.2
J	500	2000	1	0.35	12.5	1	0.5
K	125	500	1	0.35	12.5	1	0.5
L	500	0	1	0.35	12.5	1	∞
M	500	10	1	0.35	12.5	1	100
N	500	100	1	0.35	12.5	1	10
O	2500	500	1	0.35	12.5	1	10
P	500	500	1	0.35	12.5	1	2
Q	500	500	2	0.35	12.5	1	2
R	500	500	1	0.175	12.5	1	2
S	500	500	1	0.35	6.5	1	2
T	1000	1000	1	0.35	12.5	1	2
U	500	500	1	0.35	12.5	0.2	2
V	500	500	1	0.35	12.5	5	2

are investigated separately. Scalings for the one-particle diffusion in both rotation-dominated turbulence and stratification-dominated turbulence are proposed:

$$\langle\zeta_i^2(t)\rangle = \int_{t'}^t ds' \int_{t'}^{s'} \langle\dot{x}_i(s)\dot{x}_i(s')\rangle ds.$$

One popular simplifying hypothesis that has been used for computing particle diffusion is the simplified Corrsin hypothesis, which consists in replacing the Lagrangian correlation $\langle\dot{x}_i(s)\dot{x}_i(s')\rangle$ by its Eulerian counterpart. Furthermore, one can use the linear formula as an estimation for the Eulerian velocities; this is the RDT-simplified Corrsin hypothesis (SCH) method introduced in [2].

A. One-particle horizontal diffusion in stratified and rotating turbulence

For pure rotation, the formula for horizontal dispersion is given in [2] [Eq. (4.12)]:

$$\langle\zeta_h^2(t)\rangle = \frac{3}{8}\frac{u'^2}{\Omega^2} \left(4\text{Si}(2\Omega t)\Omega t + 2 \cos 2\Omega t - \frac{\sin 2\Omega t}{\Omega t} \right), \quad (28)$$

where $\text{Si}(s) = \int_0^s u^{-1} \sin u \, du$. This equation derived from the simplified Corrsin hypothesis explains the two asymptotic behaviors observed for one-particle horizontal diffusion for

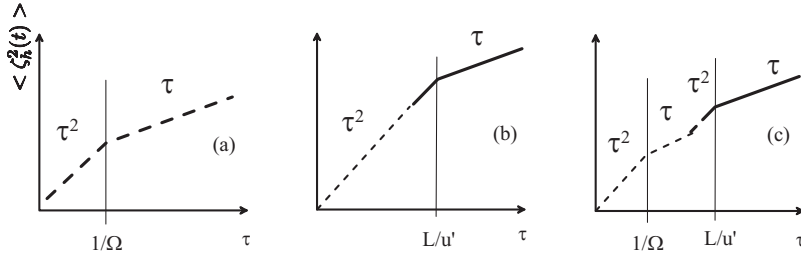


FIG. 3. Schematic scenario of superposition of rotation and stratification diffusion patterns. Dashed lines show what can be predicted by the simplified Corrsin hypothesis. (a) Pure rotation; (b) pure stratification; (c) rotation and stratification.

pure rotation: the ballistic regime when $\Omega t \rightarrow 0$ and the τ regime when $\Omega \tau \rightarrow \infty$. A similar equation can be derived for pure stratification from [2] [Eq. (4.7) with $\sigma_r=0$]:

$$\langle u_1(t)u_1(t') + u_2(t)u_2(t') \rangle = \frac{3}{2}u'^2 \int_0^1 [1 + \cos^2 \theta \cos(Nt \sin \theta) \times \cos(Nt' \sin \theta)] d \cos \theta, \quad (29)$$

that is,

$$\langle \zeta_h^2(t) \rangle = \frac{3}{2}u'^2 \left[t^2 + \int_0^1 \left(\cos^2 \theta \frac{\sin^2(Nt \sin \theta)}{N^2 \sin^2 \theta} \right) d \cos \theta \right]. \quad (30)$$

It is worth emphasizing here that Eq. (30) does not contain any information about the turbulence or nonlinear characteristic time L/u' ; so that the τ^2 regime, which is known to last up to times of the order of L/u' in the case of pure stratification, cannot be related to (30). This is why [2] concluded that the simplified Corrsin hypothesis could not be valid in cases without rotation. In the present paper analyzing the particle diffusion rather than just the velocity correlations, we can further restrict the validity of this hypothesis to pure rotation only. Furthermore, in Sec. III C we discuss whether the RDT-SCH is valid after all.

τ regimes are of very different natures in pure stratification and pure rotation.

(i) In pure stratification the τ regime is the well-known random walk or Brownian motion that appears when the particle has been diffusing for longer than the turbulence characteristic time; it is independent of N and always appears at a time that scales with L/u' .

(ii) In pure rotation the τ regime is not nonlinear or random walk by nature, it is independent of the turbulence characteristic time, and appears when the particle has been diffusing for longer than $1/\Omega$ as predicted by (28). To avoid confusion, we will refer to this regime as the rotation τ regime.

Having that picture in mind it is then easier to understand the main pattern of one-particle horizontal diffusion in a turbulent stratified and rotating flow as illustrated in Fig. 3.

The ballistic regime yielding a τ^2 law is a common feature in particle diffusion at very small times. It results from the first term of a Taylor expansion of the diffusion as discussed, for instance, in [18] for stratified turbulence.

In this regime,

$$\langle (\zeta_h^r)^2 \rangle = (u_h)^2 \tau^2, \quad (31)$$

where u_h is a velocity scale function of turbulence parameters. This common ballistic regime will end when the ballistic regime for either the stratification or the rotation is ended, that is, when

$$\tau > \min\left(\frac{L}{u'}, \frac{1}{\Omega}\right). \quad (32)$$

In the present paper, for the KS (and RDT) to be valid we need both $1/\Omega$ and $1/N \ll L/u'$, so that the ballistic regime for the rotation component will always end before the ballistic regime for the stratification component. It is then safe to assume that there will always be a ballistic τ^2 regime up to $1/\Omega$ and a random walk after L/u' . That is, after a characteristic time ignored by the simplified Corrsin hypothesis; therefore this hypothesis is not valid whenever $N > 0$.

We need now to discuss what happens when $1/\Omega < \tau < L/u'$. In Fig. 4, the horizontal diffusion results are plotted in terms of $\langle \zeta_h^2 \rangle / L^2$ as a function of τ/t_d , with $B=0.2$ in all cases. The curves collapse together, and $\langle \zeta_h^2 \rangle / L^2$ is therefore a universal function of τ/t_d , which reveals that in this stratification-dominated turbulence, the one-particle horizontal diffusion behaves in the same way as in purely stratified turbulence. This is confirmed in Fig. 5, when rotation is superimposed on stratification, but for $B < 1$ (i.e., $\Omega=0$ and 125); the one-particle horizontal diffusion barely changes its pattern from the one in purely stratified turbulence. The effect of the superimposed rotation is therefore negligible, although the tendency to have a transition τ regime between two τ^2 regimes can already be observed when B is close to 1.

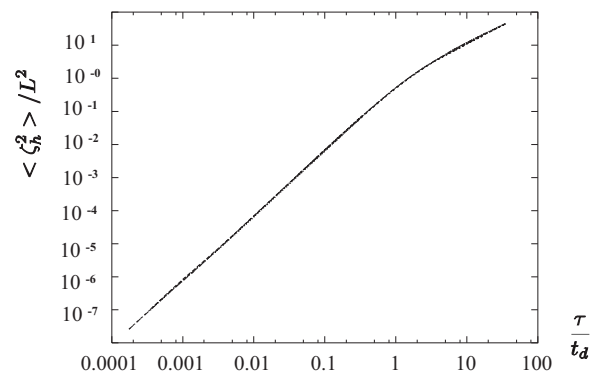


FIG. 4. Nondimensional one-particle mean square horizontal displacement $\langle \zeta_h^2 \rangle / L^2$ as a function of τ/t_d in stratification-dominant turbulence with $B=0.2$ for cases B, C, D, E, and F in Table I.

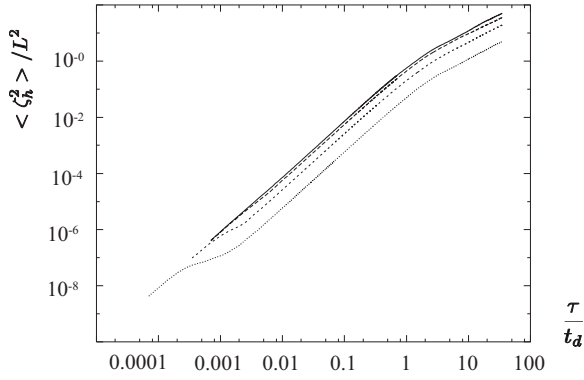


FIG. 5. Effects of rotation on stratification with $N=500$. Nondimensional one-particle mean square horizontal displacement $\langle \zeta_h^2 \rangle / L^2$ plotted as a function of τ / t_d for cases A, K, P, and O in Table I. From top to bottom $\Omega=0, 125, 500$, and 2500 .

As Ω increases and $B > 1$, the diffusion in the early ballistic τ^2 regime is not affected but this regime is shortened; it ends with the rotation ballistic regime whose length was shown to scale with $1/\Omega$. This ballistic regime is followed by a τ regime, the length of which increases with B . This τ regime is the rotation τ regime; it is not a random walk regime, and in this regime the particle has not forgotten its initial position. Thus, for longer times ($\sim 1/N$) when stratification waves develop, a pure stratification pattern—i.e., τ^2 up to L/u' and then a random walk—is superimposed onto the rotation pattern, yielding that typical feature of a τ regime in between two τ^2 regimes as sketched in Fig. 3.

Figure 5 also shows that the superimposed rotation has no effect on the starting time of the random walk τ regime. In rotation-dominated turbulence, $B=2$, the results of the horizontal diffusion are summarized in Fig. 6 with two different normalizations and in Fig. 7 for larger values of B . It is worth noting here that the two τ^2 regimes, with a transition τ regime were also observed in DNS. Reference [12] found the same results for the one-particle horizontal diffusion in rotation-dominated turbulence (i.e., $B > 1$) though the authors did not specify whether the transition regime was a τ regime. When examining their figures, one can easily see that this τ regime is the asymptotic line of the transition range. Although in Fig. 6 with $B=2$ this feature is not very evident, it becomes more noticeable when B is increased, as shown in Fig. 7.

This explains the different patterns for $B < 1$ and $B > 1$. By definition, when $B < 1$ the stratification is dominant and the mechanisms leading to the rotation structure cannot prevail so that the rotation τ regime and the second τ^2 regime are inhibited. However, when $B > 1$ the rotation is predominant and the rotation τ regime can develop. Figure 7 shows that the onset of this regime driven by rotation is not affected by N ; and Fig. 6(a) shows that it scales with $1/\Omega$.

With the normalization adopted in Fig. 6(a), all the curves collapse together in the two τ^2 regimes and the transition τ regime; therefore the nondimensional horizontal diffusion $\langle \zeta_h^2 \rangle \Omega^2 / u'^2$ in these regimes is a universal function of B and $\Omega \tau / \pi$ when $\tau \ll L/u'$. In contrast, the nondimensional horizontal diffusion $\langle \zeta_h^2 \rangle / L^2$ is found to be a universal function of

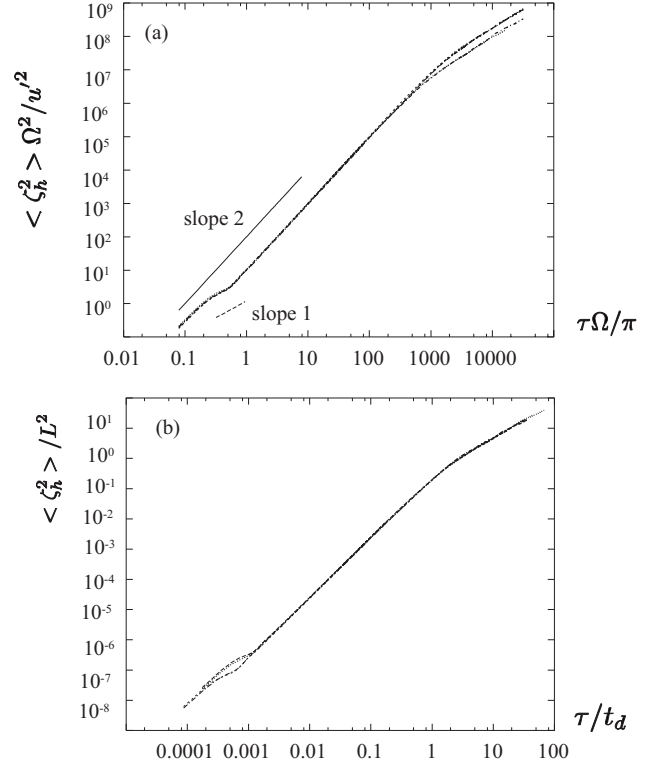


FIG. 6. One-particle mean square horizontal displacement in rotation-dominated turbulence with $B=2$ for cases P, Q, R, S, and T in Table I. (a) $\langle \zeta_h^2 \rangle \Omega^2 / u'^2$ as a function of $\tau \Omega / \pi$. (b) $\langle \zeta_h^2 \rangle / L^2$ as a function of τ / t_d .

$B\tau/t_d$ in the final random walk τ regime and the later τ^2 regime as shown in Fig. 6(b). By the way, the facts that $\langle \zeta_h^2 \rangle \Omega^2 / u'^2$ is a function of $\Omega \tau / \pi$ and that also $\langle \zeta_h^2 \rangle / L^2$ is a function of τ / t_d in this later τ^2 regime imply that $\langle \zeta_h^2 \rangle \sim (u' \tau)^2$, as already mentioned above.

The main results of having rotation superimposed on stratified turbulence can be summarized as follows.

- (1) The time when the random walk regime starts is only a function of L/u' regardless of the value of N or Ω .
- (2) As N increases (or B decreases), the transition τ regime is shortened until finally it disappears when $B < 1$.

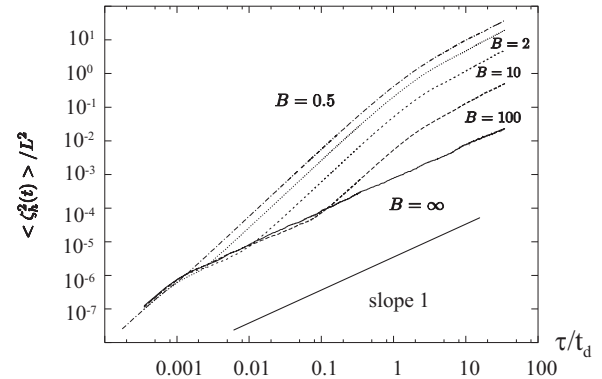


FIG. 7. Effects of stratification on rotation with $\Omega=500$. Nondimensional one-particle mean square horizontal displacement $\langle \zeta_h^2 \rangle / L^2$ plotted as a function of τ / t_d for cases J, P, N, M, and L in Table I. From top to bottom $N=2000, 500, 100, 10$, and 0 .

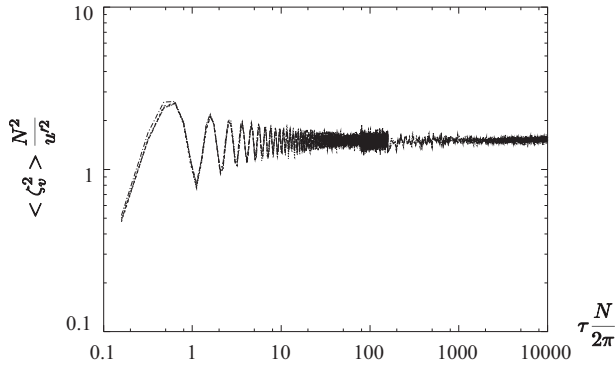


FIG. 8. Nondimensional one-particle mean square vertical displacement $\langle \zeta_3^2 \rangle N^2 / u'^2$ as a function of $\tau N / 2\pi$ in stratification-dominant turbulence with $B=0.2$ for (from top to bottom) cases B, C, D, E, and F in Table I.

- (3) The diffusion after the ballistic τ^2 regime increases when B decreases.
- (4) No effect of the superimposed stratification on the diffusion in the ballistic τ^2 regime is observed, and this regime finishes at a time related to Ω only.

B. One-particle vertical diffusion in stratified and rotating turbulence

From Fig. 8 where B equals 0.2, one can see that the nondimensional vertical diffusion $\langle \zeta_3^2 \rangle N^2 / u'^2$ is a universal function of $(N/2\pi)\tau$, which shows that the one-particle vertical diffusion in this turbulence also behaves as in purely stratified turbulence. The diffusion pattern does not change very much; the difference is hardly discernible apart from the first loop of the oscillations, where the diffusion sometimes shows higher or lower values than in the case without rotation.

The superimposed rotation makes a distinctive difference only when the turbulence becomes rotation dominated, $B > 1$. Figure 9 shows that, as Ω increases, the amplitude of the plateau is reduced; moreover, the starting time of the plateau is moved forward. It is also observed that rotation has no significant influence on the diffusion in the ballistic τ^2 regime except that the regime is shortened as Ω increases.

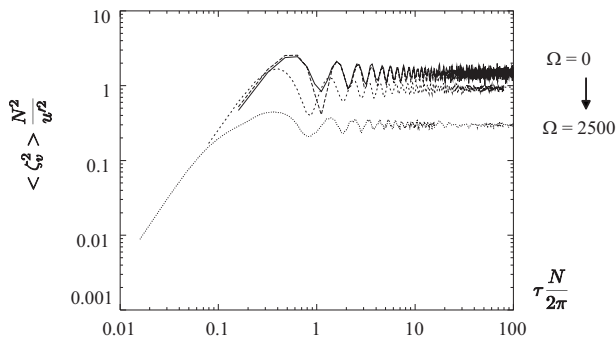


FIG. 9. Effects of rotation on stratification with $N=500$. Nondimensional one-particle mean square vertical displacement $\langle \zeta_3^2 \rangle N^2 / u'^2$ plotted as a function of $\tau N / 2\pi$ for the same cases as in Fig. 5. From top to bottom $\Omega=0, 125, 500$, and 2500.

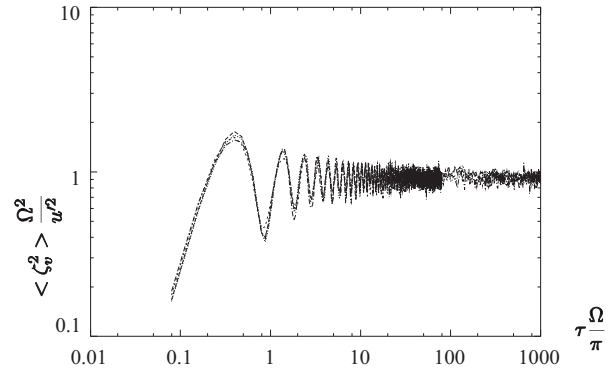


FIG. 10. Nondimensional one-particle mean square vertical displacement $\langle \zeta_3^2 \rangle \Omega^2 / u'^2$ as a function of $\tau \Omega / \pi$ in rotation-dominant turbulence with $B=2$ for (from top to bottom) cases P, Q, R, S, and T in Table I.

The results for the vertical diffusion when $B=2$ are shown in Fig. 10. The curves plotted as they are in this figure show a good collapse in this rotation-dominated turbulence case. Minor differences appear at the early stage of oscillations which only weakly affect the normalization around the crests of the first few oscillation periods. Thus the nondimensional vertical diffusion $\langle \zeta_3^2 \rangle \Omega^2 / u'^2$ is a universal function of $\Omega \tau / \pi$ and B in rotation-dominated turbulence.

Furthermore, Fig. 11 shows that the Coriolis term does not affect the existence of a vertical diffusion capping, though it affects the value of the plateau. This is expected as the analysis conducted in [3,19] in terms of potential energy is still valid (Coriolis force has no work), thus implying a plateau for vertical diffusion which must scale as

$$\langle \zeta_3^2 \rangle \approx f(B) \frac{u'^2}{N^2}. \tag{33}$$

Even with a relatively weak stratification, that is, $B=100$, for large times the diffusion pattern has been changed into a pure stratification pattern with a capping of the diffusion in the vertical direction. However, at smaller times it does not faithfully behave as in pure stratification. Instead, it contains an

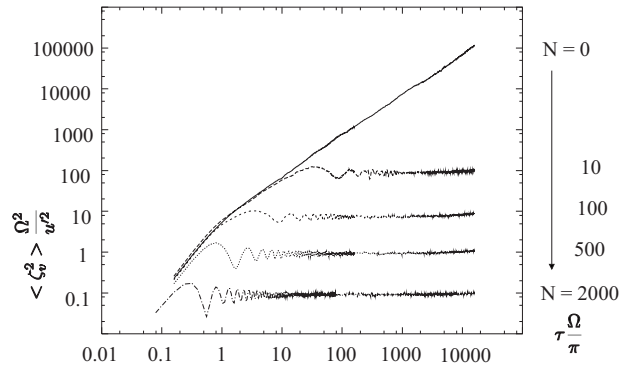


FIG. 11. Effects of stratification on rotation with $\Omega=500$. Nondimensional one-particle mean square vertical displacement $\langle \zeta_3^2 \rangle \Omega^2 / u'^2$ plotted as a function of $\tau \Omega / \pi$ for the same cases as in Fig. 7. From bottom to top $N=2000, 500, 100, 10$, and 0.

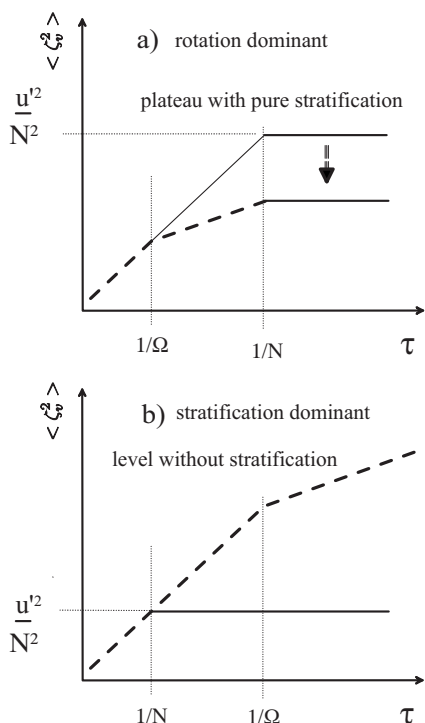


FIG. 12. Schematic scenario of one-particle diffusion when rotation and stratification are superposed. (a) For $B > 1$ the rotation pattern settles first and the stratification characteristic plateau appears afterward. (b) For $B < 1$ the stratification plateau appears before the rotation effects start, so that the rotation does not affect the plateau.

additional transition τ regime between the ballistic τ^2 regime and the final plateau.

The beginning of the plateau is governed by the stratification and scales with $1/N$, whereas the transition τ regime, as already mentioned for the horizontal diffusion, is an effect of the rotation and its beginning scales with $1/\Omega$ provided that both effects can coexist, that is, $1/\Omega < 1/N$ or $B > 1$. As N increases, the rotation τ regime decreases until it completely disappears when $B < 1$, and the diffusion then follows a pure stratification pattern. Meanwhile, the amplitude of the plateau is decreased as N increases.

It is important to point out here the reason why turbulent parameter values such as $\Omega = 500$, $L = 1$, and $u' = 0.35$ (that is, $Ro = 0.00035$) have been chosen in this study. In rotating turbulence with weak stratification, e.g., $B = Fr/Ro = 100$, the diffusion in the vertical direction behaves as in pure stratification. Only with very small values of the Rossby number can one have small enough Froude numbers to make valid the RDT on which our KS model is based.

Figure 12 describes the effect of rotation on the vertical diffusion.

(1) In any case, as already mentioned for $N\tau \gg 1$, a plateau is observed in accordance with the principle of energy conservation.

(2) A ballistic regime is observed when both stratification and rotation ballistic regimes coexist, that is, up to $\tau = \min(\Omega^{-1}, N^{-1})$.

(3) When stratification is dominant ($B < 1$), the plateau is reached before the rotation waves can develop, so that the

rotation has no effect on the vertical diffusion.

(4) When rotation is dominant ($B > 1$), the rotation τ regime develops before stratification waves so that the plateau is lowered and is a function of both Ω and N .

C. Is RDT-SCH valid after all?

We have seen that the RDT-SCH is not valid whenever there is some stratification. This is because the Brownian motion that exists in the horizontal direction is not predicted in the RDT-SCH. In the light of this shortcoming, it is worth looking back at what was meant here earlier or in [2,14] when it was said that the SCH is valid for pure rotation. The criterion was the comparison with Lagrangian DNS results: the SCH is valid in the sense that it predicts the right Lagrangian results.

But superimposing rotation and stratification has made it clear that there are two t regimes corresponding to two different physics: one due to the wave dynamics (at small times), and one corresponding to an actual Brownian motion due to velocity decorrelation (at large times). The SCH has only one of the two physics, so it is not in that sense valid, because one would expect velocity decorrelation to occur eventually in a turbulent regime, and actual Brownian motion to exist even with pure rotation.

It is just fortunate that in Lagrangian terms it is not possible, in pure rotation, to discriminate between the two mechanisms. The first mechanism (wave dynamics) is not valid after a turnover time and should be replaced by a Brownian mechanism. The two wrongs of the SCH, not having any information about the Brownian mechanism and carrying on the first mechanism after the turbulence turnover time (or decorrelation), make a right, and in Lagrangian terms the SCH prediction is accurate.

The case $B = 1$ is illuminating in that respect, as it can show that the Brownian mechanism is always there, even in the vertical direction when there is stratification. Indeed, for $B = 1$ there is no phase mixing and results in [14] show that there is an effect of the nonlinear terms. In this case, there is a discrepancy between the RDT-SCH and DNS or KS. The discrepancy between DNS and RDT-SCH results indicates the presence of the velocity decorrelation, which cannot be discriminated from phase mixing in other cases. The comparison with the KS also shows that the KS does incorporate the velocity decorrelation. (However, in [14] the DNS and KS seem to lose their accuracy at $t > L/u'$, as then the vertical diffusion increases, whereas according to the energy argument it should be constant for ever.)

D. Role of spatial structures

KS for stratified turbulence as it is generated in this paper (Sec. II) does not contain any information about spatial structures such as layers or columns, which are observed, respectively, for stratified turbulence and rotating turbulence. Recent and higher-resolution results of such structures can be found in [14]. So how important are these structures in the prediction of particle diffusion? First, what matters in Lagrangian tracking is Lagrangian correlations not Eulerian ones. So it is necessary to get accurate Lagrangian velocity

correlations. Comparisons with DNS [2,14] show that the KS without the Eulerian structures predicts accurately the diffusion for one and two particles for stratified, rotating, and stratified and rotating turbulence.

We refer the reader to [14] for a detailed analysis of the small impact of spatial structures on the particle diffusion. Here, we want to emphasize that layered structures cannot explain the main feature of diffusion in stratified turbulence, which is that the vertical diffusion exhibits a plateau when $N\tau > 1$. Indeed, the energy argument that $N^2 \langle \zeta^2(\tau) \rangle$ must be bounded is valid with or without rotation, as the Coriolis force does not work. Therefore, whatever the finite value of B , there exists a plateau irrespective of whether the Eulerian spatial structures are predominantly layerlike or columnlike, or neither when $B=1$.

We can conclude that linear time oscillations that are contained in KS are necessary and sufficient to predict accurately particle diffusion in stratified and/or rotating turbulence, whereas Eulerian structures such as layers or columns are neither sufficient nor necessary.

IV. TWO-PARTICLE DIFFUSION IN STRATIFIED AND ROTATING TURBULENCE

In this section, two-particle diffusion is investigated when there is stratification and rotation. We do not discuss here the capacity of KS to model two-particle diffusion in general. In particular, we do not comment on the effect of having no explicit sweeping mechanism in our model. The validity of our results is supported by previous research, e.g., [10,21], for two-particles and in [20,22], where KS and experimental results of multiparticle diffusion are compared. All these studies support the use of KS when $L/\eta < 10^4$ (in this paper $L/\eta < 100$). As to the reasons for extending an isotropic hypothesis (Richardson's) to stratified and rotating turbulence, we refer the reader to the discussion in [1].

Pair diffusion has been studied in [1] for the cases of pure rotation and pure stratification; in this paper, we study the combined effect of both rotation and stratification. It is hard, without an energy argument to use or DNS results at large Reynolds number to compare with, to estimate the role the Eulerian structures could have in pair diffusion. For vertical diffusion, when there is stratification, we are quite confident from our comparison with [12] that the effect is negligible. When it comes to pair diffusion in the horizontal direction (or along any direction for pure rotation), one wants to see a Richardson regime and compare power laws. It is worth noting in this context that there are already arguments as to whether one can find a Richardson regime in an isotropic DNS. So we could conclude from the fact that we do not observe discrepancy between KS and DNS pair diffusion for the cases in [12] that the Eulerian structures are not important for two-particle dispersion, at least for the Reynolds numbers achievable in DNS.

Figures 13 and 14 summarize the diffusion results in stratified and rotating turbulence for the two different values of $B=0.2$ and 2. Each figure shows a particular aspect of the diffusion at a given value of B .

Features shared in the same range of time by purely rotating and purely stratified turbulence are also observed

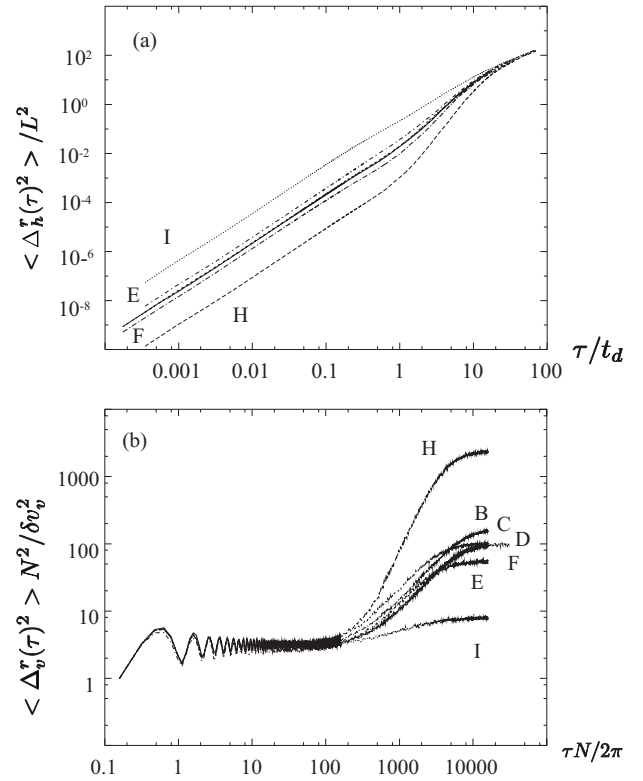


FIG. 13. Nondimensional pair mean square relative horizontal separation when $B=0.2$ for cases B, C, D, E, F, H, and I in Table I. (a) $\langle \Delta_h^r(\tau)^2 \rangle / L^2$ as a function of τ/t_d . (b) $\langle \Delta_v^r(\tau)^2 \rangle N^2 / \delta v_v^2$ as a function of $\tau N / 2\pi$.

when both are acting on turbulence. In particular, there is an early-time ballistic τ^2 regime:

$$\langle \Delta_i^r(\tau)^2 \rangle = \delta v_i^2 \tau^2.$$

It can be seen that, when $B=0.2$, the two-particle diffusion in this stratification-dominated turbulence displays no significant difference from that in purely stratified turbulence in both the horizontal plane and the vertical direction.

However, when $B=2$, the leading effect of the rotation in horizontal diffusion is to generate a transition τ regime and a

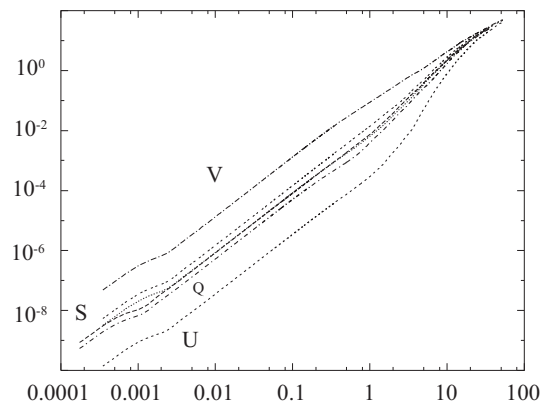


FIG. 14. Nondimensional two-particle mean square relative horizontal separation with $B=2$ for cases P to V in Table I. $\langle \Delta_h^r(\tau)^2 \rangle / L^2$ as a function of τ/t_d (middle curves: cases P, R, and T).

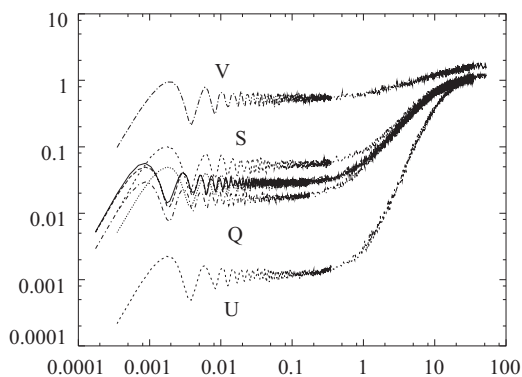


FIG. 15. Nondimensional two-particle mean square relative vertical separation, $\langle(\Delta_3^r)^2\rangle/L^2$, as a function of τ/t_d with $B=2$ for cases P to V in Table I (middle curves: cases P, R, and T).

later τ^2 regime different from the early-time ballistic τ^2 regime. Nevertheless, the diffusion in the vertical direction behaves as in purely stratified turbulence, i.e., there are two plateaus in the vertical diffusion (not shown here).

In the final τ regime as shown in Figs. 13 and 14 the nondimensional mean square horizontal diffusion $\langle\Delta_h^r(\tau)^2\rangle/L^2$ is found to be a universal function of τ/t_d for both $B=0.2$ and $B=2$. The two-particle horizontal diffusion at intermediate times is found to be governed by the locality-in-scale hypothesis. This is investigated in Sec. IV D.

With respect to two-particle diffusion in the vertical direction, as shown in Fig. 15, the scalings of the first and the second plateaus are based on the same parameters as in purely stratified turbulence, except that the coefficients in these scalings now depend on the value of B .

A. Effects of superimposed stratification on pair horizontal diffusion in turbulence with constant Ω

Figure 16 presents the effects of superimposed stratification on two-particle horizontal diffusion at a fixed value of Ω . Before the pair enters the intermediate range of time where a Richardson's law could develop, observations simi-

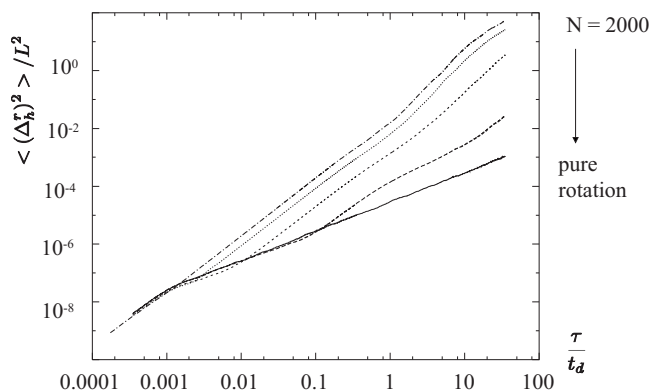


FIG. 16. Effects of stratification on rotation with $\Omega=500$. Nondimensional two-particle mean square relative separation in horizontal plane, $\langle(\Delta_h^r)^2\rangle/L^2$, plotted as a function of τ/t_d for cases L, M, N, P, and J in Table I. From top to bottom $N=2000, 500, 100, 10$, and 0.

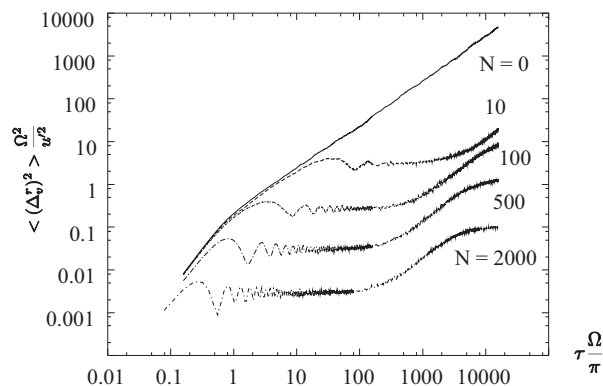


FIG. 17. Effects of stratification on rotation with $\Omega=500$. Nondimensional two-particle mean square relative separation in vertical direction, $\langle(\Delta_v^r)^2\rangle\Omega^2/u'^2$, plotted as a function of $\tau\Omega/\pi$ for the same cases as in Fig. 16. From bottom to top $N=2000, 500, 100, 10$, and 0.

lar to the ones made for one-particle diffusion (Fig. 7) can now be made for the pair horizontal diffusion.

One can see from Fig. 16 that the superimposed stratification does not affect the diffusion in the ballistic τ^2 regime, but as N increases the diffusion is enhanced in the subsequent regimes compared with the case without stratification. Furthermore, as the stratification gets stronger, the transition τ regime becomes shorter until it finally disappears or is hardly observed when the stratification becomes dominant.

The final random walk τ regime for the two-particle diffusion can be observed only when the stratification is strong (see Fig. 16). As N decreases, this regime is delayed and could not be reached for $B \geq 10$. As a result the diffusion at intermediate times is not displayed completely. Since the Rossby number considered here is very small, $Ro = 0.00035$, it would require a much longer simulation time to reach the final random walk regime.

B. Effects of superimposed stratification on pair vertical diffusion in turbulence with constant Ω

In the vertical direction, Fig. 17 shows that even a very weak stratification can lead to a diffusion pattern dramatically different from the one in purely rotating turbulence. After a certain time the diffusion is capped and a plateau appears, as it would for pure stratified turbulence. If N is large enough, a second plateau can also be observed.

The figure also shows that, when N is very small, that is, $B \gg 1$, the diffusion behaves as in pure rotation for a certain period of time, with a τ regime followed by the first plateau. When rotation is an overwhelmingly dominant factor of the turbulence, the ballistic τ^2 regime finishes at a time independent of N but a function of Ω . Nevertheless, the times when the first plateau starts and stops are determined by N rather than Ω ; a smaller N corresponds to a later appearance and a later termination of the first plateau.

As N increases the τ regime gets shorter until it finally disappears when the stratification becomes dominant, and the diffusion then follows a pure stratification pattern. Furthermore, an increment of N only slightly reduces the diffusion

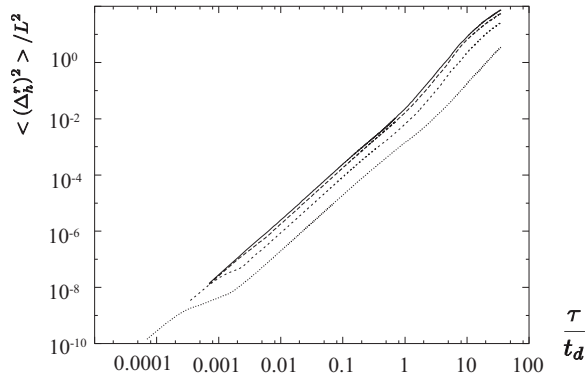


FIG. 18. Effects of rotation on stratification with $N=500$. Non-dimensional two-particle mean square relative separation in horizontal plane, $\langle (\Delta_h')^2 \rangle / L^2$, plotted as a function of τ / t_d for cases A, K, P, and O in Table I. From top to bottom $\Omega=0, 125, 500$, and 2500.

in the ballistic τ^2 regime but considerably decreases the levels of the two plateaus.

With the parameters chosen here, one can only observe the second plateau in the case of $N=2000$. Provided that enough computation time is available, the second plateau can be obtained for all the cases except $N=10$, as in this case the Froude number is not small enough to make the KS model valid for such a long time.

C. Effects of superimposed rotation on diffusion in turbulence with constant N

Figures 18 and 19 illustrate the effects of superimposed rotation on the two-particle diffusion in turbulence with a fixed value of N . In the horizontal diffusion, if the rotation is weak, that is, $B < 1$, the diffusion is slightly affected. As Ω increases, a more obvious transition τ regime arises and shifts to an earlier time. In the meantime, the diffusion is reduced, and the final τ regime is postponed until there is no such regime observed in the case of $\Omega=2500$. It is also shown that the introduction of rotation has no effect on the diffusion in the ballistic τ^2 regime but shortens it; further-

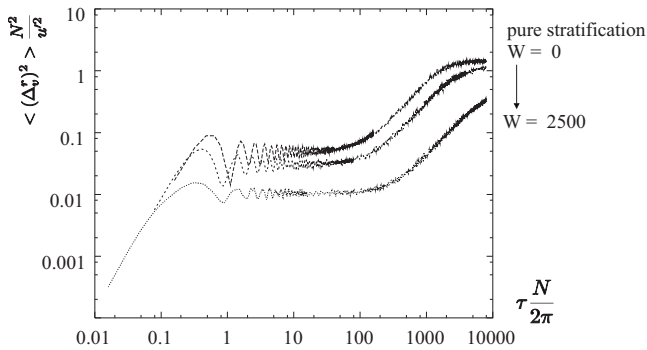


FIG. 19. Effects of rotation on stratification with $N=500$. Non-dimensional two-particle mean square relative separation in vertical direction, $\langle (\Delta_v')^2 \rangle N^2 / u'^2$, plotted as a function of $\tau N / 2\pi$ for the same cases as in Fig. 18. From top to bottom $\Omega=0, 125, 500$, and 2500.

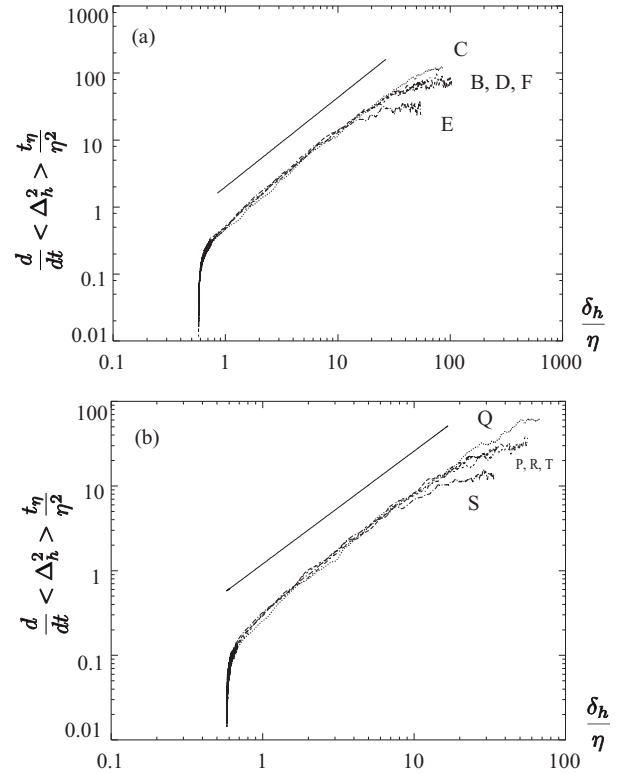


FIG. 20. Nondimensional two-particle horizontal diffusivity $(d/dt)\langle \Delta_h^2 \rangle t_\eta / \eta^2$ as a function of δ_h / η . The solid line represents Richardson's four-thirds diffusivity law. (a) $B=0.2$ for cases B to F in Table I. (b) $B=2$ for cases P to T in Table I.

more, the later τ^2 regime also finishes at a time independent of Ω but a function of L/u' .

As for the diffusion in the vertical direction, it is shown that a weak rotation cannot alter the diffusion very much until it becomes dominant over stratification, i.e., $B > 1$. As Ω increases, the diffusion in the ballistic τ^2 regime is not affected significantly; by contrast the levels of the two plateaus are further decreased. Meanwhile, the first plateau starts earlier but finishes at a later time, and as a consequence the second plateau's appearance is postponed.

D. Investigation of the locality-in-scale hypothesis

As shown in Figs. 20 and 21, the two-particle horizontal diffusion in the intermediate range of times is found to be governed by Richardson's four-thirds diffusivity law. For a given value of B , Richardson's coefficient β_h is an increasing function of Δ_0 / η , and the law is valid in a range determined by L/η and Δ_0/η .

Here as well the identical effects of stratification and rotation on turbulence pair diffusion will be retrieved when both are present at the same time. In particular, whatever the value of B , rotation and stratification's overall effect is to decrease the diffusion and improve the locality assumption.

More can be deduced about the locality-in-scale hypothesis and Richardson's diffusivity law in rotating and stratified turbulence. It can be seen that, in Fig. 20, at a fixed value of B and Δ_0/η , all the curves collapse to the line representing

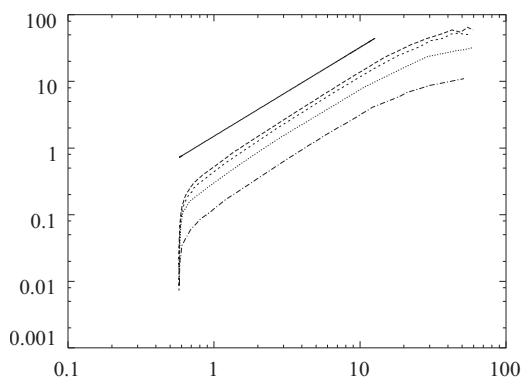


FIG. 21. Effects of B on two-particle diffusivity in rotating and stratified turbulence. Nondimensional horizontal diffusivity $\langle \Delta_h^2 \rangle t_\eta / \eta^2$ plotted as a function of δ / η . From top to bottom $B = 0, 0.5, 2,$ and 10 . Other parameters are $L=1, 1/\eta=12.5, u' = 0.35,$ and $\Delta_0/\eta=1$. Solid line has a slope of $4/3$, representing Richardson's four-thirds diffusivity law.

Richardson's four-thirds diffusivity law regardless of the turbulence parameters $L, u', \eta, N,$ and Ω . This means that, at a given B and Δ_0/η , Richardson's coefficient β_h does not depend on the turbulence parameters, whereas the range χ_h depends on L/η .

Figure 22 shows the effect of the initial separation on β_h for $B=0.2$ and 2 . Whether B equals 2 or 0.2 , for a given value of Δ_0/η , the variation of β_h in Richardson's four-thirds range is negligible; it can hence be treated as a δ -independent coefficient that increases with Δ_0 . The locality-in-scale hypothesis then applies to any initial separation. It can also be seen that χ_h decreases with increasing Δ_0/η when $\Delta_0/\eta > 1$.

Comparing Figs. 20(a) and 20(b), that is, $B=0.2$ and 2 , one can see that the value of β_h differs, which implies that at a constant Δ_0/η , β_h is only a function of B .

As shown in Fig. 21, as B increases the value of β_h is reduced compared with the case without rotation. However B has no significant effect on χ_h .

So, to summarize, Richardson's coefficient β_h is Δ_0 dependent. Its value increases with Δ_0/η but decreases with B . While χ_h is independent of B and determined by L/η and Δ_0/η , it increases with L/η and decreases with Δ_0/η when $\Delta_0/\eta > 1$.

V. CONCLUSION

In this paper, we use KS coupled with rapid distortion theory to model one- and two-particle diffusion in turbulence with stratification and rotation. We show that the simplified Corrsin hypothesis introduced in [2] has to be restricted to pure rotation only.

One-particle and two-particle diffusion is investigated in the horizontal and vertical directions. For one-particle hori-

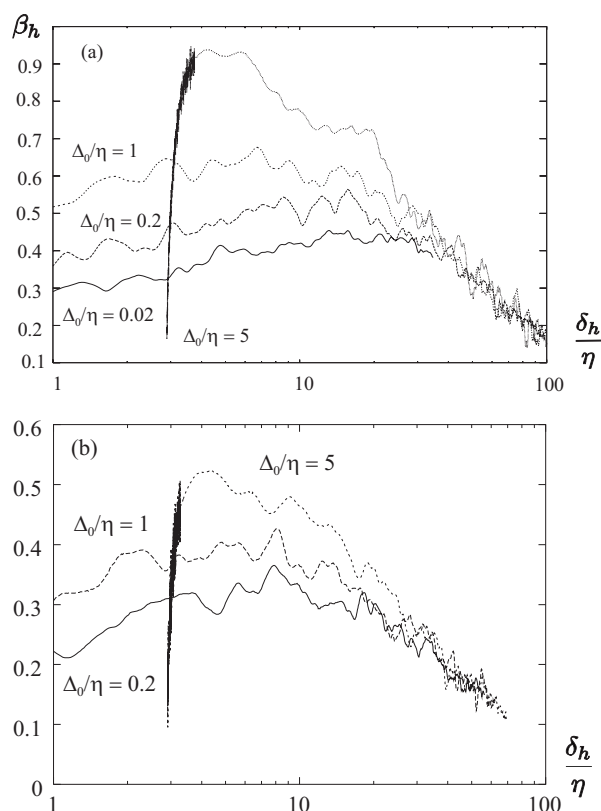


FIG. 22. β_h as a function of δ_h : (a) $B=0.2$ for cases B, G, H, and I in Table I; (b) $B=2$ for cases P, U, and V in Table I.

zontal dispersion we observe four regimes: the ballistic regime when $\tau < 1/\Omega$; an intermediary τ regime which is not the random walk; followed by a τ^2 regime up to $\tau \approx L/u'$; and finally the random walk τ regime when $\tau > L/u'$

For one-particle vertical diffusion, the effect of rotation is to lower the diffusion's plateau. A plateau is always observed as soon as there is stratification, in accordance with the principle of energy conservation. We conclude that the Eulerian spatial structure that exists in real flows but not in KS plays a minor role in the vertical capping observed in stratified flows.

When considering two-particle diffusion, adding rotation to stratification has the same effect in the ballistic regime as is observed for one-particle diffusion. That is, it introduces an intermediary τ regime which delays all the subsequent regimes.

We analyze the locality-in-scale hypothesis in the intermediary range of times and adopt [10]'s approach to study β_h as a function of δ_h/η . We conclude that β_h does not depend on the turbulence's parameters but on B , whereas, χ_h , the range over which β_h is close to a constant, is independent of B and is a function of the turbulence's parameters.

F.N. and G.Y. acknowledge EPSRC Grant No. GR/N22601, EPSRC U.K. Turbulence Consortium, and Grant No. GR/R64957/01.

- [1] F. Nicolleau, G. Yu, and J. C. Vassilicos, *Fluid Dyn. Res.* (to be published).
- [2] C. Cambon, F. S. Godeferd, F. Nicolleau, and J. C. Vassilicos, *J. Fluid Mech.* **499**, 231 (2004).
- [3] F. Nicolleau and J. C. Vassilicos, *J. Fluid Mech.* **410**, 123 (2000).
- [4] J. C. H. Fung, J. C. R. Hunt, N. A. Malik, and R. J. Perkins, *J. Fluid Mech.* **236**, 281 (1992).
- [5] F. W. Elliott and A. J. Majda, *Phys. Fluids* **8**, 1052 (1996).
- [6] J. C. H. Fung and J. C. Vassilicos, *Phys. Rev. E* **57**, 1677 (1998).
- [7] N. A. Malik and J. C. Vassilicos, *J. Fluid Mech.* **326**, 417 (1996).
- [8] P. Flohr and J. C. Vassilicos, *J. Fluid Mech.* **407**, 315 (2000).
- [9] F. Nicolleau and A. ElMaihy, *J. Fluid Mech.* **517**, 229 (2004).
- [10] F. Nicolleau and G. Yu, *Phys. Fluids* **16**, 2309 (2004).
- [11] Y. Kaneda and T. Ishida, *J. Fluid Mech.* **402**, 311 (2000).
- [12] Y. Kimura and J. R. Herring, in *Proceedings of FEDSM99* (ASME, San Francisco, 1995).
- [13] F. S. Godeferd and C. Cambon, *Phys. Fluids* **6**, 2084 (1994).
- [14] L. Liechtenstein, C. Cambon, and F. Godeferd, *J. Turbul.* **6**, 1 (2005).
- [15] A. M. Obukhov, *Bull. Acad. Sci. USSR, Geogr. Geophys.* **5**, 453 (1941).
- [16] G. K. Batchelor, *Proc. R. Soc. London, Ser. A* **213**, 349 (1952).
- [17] P. Morel and M. Larchevêque, *J. Atmos. Sci.* **31**, 2189 (1974).
- [18] F. Nicolleau and J. C. Vassilicos, *Phys. Rev. Lett.* **90**(2), 024503 (2003).
- [19] H. Hanazaki and J. C. R. Hunt, *J. Fluid Mech.* **318**, 303 (1996).
- [20] M. A. I. Khan, A. Pumir, and J. C. Vassilicos, *Phys. Rev. E* **68**, 026313 (2003).
- [21] D. R. Osborne, J. C. Vassilicos, K. Sung, and J. D. Haigh, *Phys. Rev. E* **74**, 036309 (2006).
- [22] F. Nicolleau and A. ElMaihy, *Phys. Rev. E* **74**, 046302 (2006).